



# **Congo Red Removal from Polluted Water using NaOH Treated Fallen Leaves of *Ficus racemosa***

**G. Indramahalakshmi<sup>a\*</sup>**

<sup>a</sup> *Department of Chemistry, Cardamom Planters' Association College, Bodinayakanur-625513, Tamil Nadu, India.*

## **Author's contribution**

*The sole author designed, analysed, interpreted and prepared the manuscript.*

## **Article Information**

DOI: 10.9734/AJOCS/2024/v14i2292

## **Open Peer Review History:**

This journal follows the Advanced Open Peer Review policy. Identity of the Reviewers, Editor(s) and additional Reviewers, peer review comments, different versions of the manuscript, comments of the editors, etc are available here: <https://www.sdiarticle5.com/review-history/113844>

**Original Research Article**

**Received: 01/01/2024**

**Accepted: 06/03/2024**

**Published: 12/03/2024**

## **ABSTRACT**

Naoh treated biosorbent *Ficus Racemosa* Leaf Powder (NaFRLP) was prepared from the fallen leaves of the plant. FT-IR, SEM and BET analysis were done to characterize the biosorbent. The biosorbent was found to be mesoporous with an average pore size 18 nm. Batch adsorption equilibrium studies were conducted for the adsorption of congo red on NaFRLP as a function of adsorbent dosage, agitation speed, dye concentration, temperature and contact time. Batch adsorption studies revealed that with an increase in the time of adsorption, the percentage removal of congo red increases and with an increase in the concentration of dye solution, congo red removal decreases. Initial dye concentration of 100 mgL<sup>-1</sup>, agitation speed 200 rpm and adsorbent dosage 1gL<sup>-1</sup> were the optimum conditions for the effective removal of congo red. The adsorption data well agreed with the Langmuir isotherm as indicated by the higher correlation coefficient ( $R^2=0.962$ ) value. Thermodynamic analysis of the batch adsorption studies indicated that all the processes studied were spontaneous with the congo red adsorption on NaFRLP being endothermic. Intra particle diffusion model was also tested. NaFRLP was found to be an effective adsorbent for the removal of congo red from the polluted water.

\*Corresponding author: E-mail: [indramahalakshmi.g@cpacollege.org](mailto:indramahalakshmi.g@cpacollege.org);

**Keywords:** Congo red; *Ficus racemosa*; thermodynamic; isotherm; SEM; BET; thermodynamic analysis; diffusion model; cancer.

## 1. INTRODUCTION

The dye wastes from industries cause diseases like cancer, mutations, skin problems, allergic eczema etc., in mammals. The dyes cause environmental pollution such as decrease in dissolved oxygen, reduction of photosynthesis which in turn affect amphibians and plants and adverse effect on food cycle. It is mandatory to remove dye from industrial effluents.

Adsorption is an emerging and promising technique for dye removal. It has been discovered that activated carbon is a flexible adsorbent that can eliminate a wide range of contaminants, including metal ions, dyes, phenols and several other organic and inorganic substances as well as microorganisms. Attempts are being undertaken to renew the used activated carbon using chemical and thermal means due to the increased expense of activated carbon. These techniques, however, are not inexpensive and result in significant adsorbent loss as well as the production of extra effluents.

The biosorption technique is a popular biotechnological method for eliminating most heavy metals and dyes from aqueous solutions. It uses biomass that is either waste or naturally plentiful. Ion exchange resins are the closest analog for biosorption and biosorbents are sometimes called natural ion exchangers [1]. "A low cost of biosorbents, high selectivity and efficiency for dye removal at low concentrations, the potential for biosorbent regeneration, high sorption and desorption velocities, limited generation of secondary residues and a more

environmentally friendly material life cycle are the main motivators for the development of biosorption for industrial processes" [2].

"The main components of plant leaves are made up of cellulose, hemicellulose, pectins, lignin, etc.," [3]. "These substances can interact with the functional groups of dyes because they contain a variety of functional groups, including carboxyl, hydroxyl, carbonyl, amino and nitro" [4]. "Dyes bind to the biomass of leaves as a result of this interaction" [5-7]. "*Ficus racemosa* plant parts have already been used as biosorbents for the removal of dyes, metal and non metal ions" [7-9]. "Earlier studies for the removal of congo red from textile waste water using various biosorbents like leaf, fruit shell, fly ash, tea waste etc., have been reported" [10-13].

It was therefore desired that biosorbents as alternative raw materials be chosen that are region specific, easily available, inexpensive and without much commercial applications. In the present study, congo red identified for adsorption on to NaOH treated *Ficus racemosa* fallen leaf powder (NaFRLP). Batch studies were carried out in order to examine the potential of this adsorbent for adsorption of dyes from solution.

Sodium salt of 3, 3'-([1,1'-biphenyl]-4,4'-diyl) bis (4-aminonaphthalene-1-sulfonic acid) is known as Congo red. It is being studied as a potential mutagen, carcinogen and reproductive effector. It irritates the skin, eyes and digestive system. It may cause sleepiness, breathing issues and disruptions to blood components including clotting [14].



**Fig.1. *Ficus racemosa* Leaves**

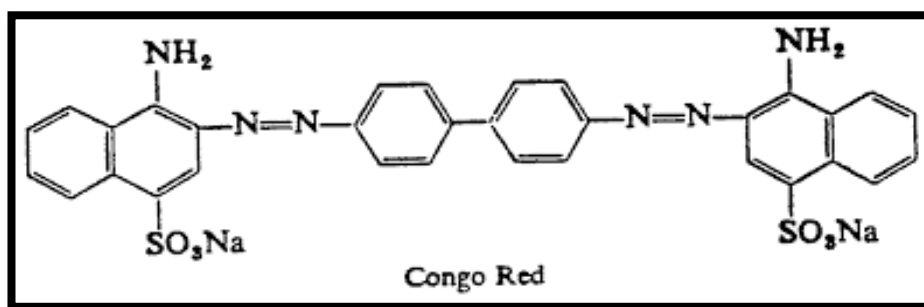


Fig. 2. Structure of Congo red

## 2. MATERIALS AND METHODS

### 2.1 Chemicals Used

Congo red was purchased from Merck and NaOH of analar grade was utilized.

### 2.2 Preparation of Biosorbent

*Ficus racemosa* leaves used in this study was collected from Theni. It was washed with double-distilled water to remove any unwanted particles and dried in an air oven at 70°C for 24 hours. The raw biosorbent was then crushed and ground using ball mill and sieved to get uniform size (150-mesh) particles. *Ficus racemosa* leaf powder (FRLP) was treated with 2% NaOH in the ratio 1:5 under stirring speed 400 rpm for about half an hour at 40°C. The NaOH treated biosorbent (NaFRLP) was washed several times with distilled water and dried naturally. NaOH treatment helps in the removal of lignin from the biomass, thus creating porous material. The particles were then stored in sealed glass containers and used in all the adsorption experiments.

### 2.3 Methods used to Characterize Biosorbent

Fourier Transform Infrared Spectroscopy (FT-IR) and Scanning Electron Microscopy (SEM) studies were used to analyze the biosorbent. Nitrogen adsorption-desorption isotherms, obtained at 77 K using the Quanta chromium Autosorb 1C system, were used to calculate the pore volumes and adsorption/desorption isotherms of the adsorbents. The samples were vacuum-degassed at 200°C prior to the commencement of N<sub>2</sub> adsorption. The BET equation and the Barret–Joyner–Halenda (BJH) method were used to calculate the surface area

and pore volumes, also known as pore size distribution.

### 2.4 Batch Adsorption Studies

The adsorption of congo red on NaFRLP was studied using batch adsorption equilibrium studies, whereby the adsorbent dose, agitation speed, dye concentration, temperature and contact duration were varied. This was accomplished by combining 300 ml of 0.1 M adsorbate solution with 1 g/L of adsorbent in a conical flask. The mixture was then stirred on a magnetic stirrer over a hot plate at 313 K for 90 minutes. Several adsorbent doses of 0.1, 0.3, 0.7, 1, 1.5 and 2 g/L were added to each conical flask holding 300 ml of 0.1 M adsorbate solution and were swirled for 90 minutes in order to assess the effects of adsorbent dosage. Each conical flask holding 300 ml of adsorbate solutions at various concentrations of 100, 200, 300, 400, 500, 600, 700 and 800 mg/L was supplemented with 1 g/L of adsorbent based on the influence of dye concentration and the mixture was swirled for 90 minutes. 300 ml of 0.1 M adsorbate solution was mixed with 1 g/L of adsorbent and stirred at intervals of 15, 30, 45, 60, 75 and 90 minutes, depending on the impact of contact time. In addition, the solution was taken out of the reaction mixture and filtered using Whatman No. 1 filter paper at a predetermined interval. Using a JASCO UV-visible spectrophotometer set to 498 nm for congo red, the amount of unadsorbed dye in the supernatant solutions was determined. The percentage of adsorption, the amount of adsorption at equilibrium ( $q_e$ ) (mg/g) and the amount of adsorption were then calculated.

$$q_e = [(C_0 - C_e) V/M] \text{ ----- (1)}$$

$$\text{Adsorbed dye percentage} = [(C_0 - C_e)/C_0] \times 100 \text{ -} \text{----- (2)}$$

Where,

$C_0$  and  $C_e$  are the initial and final dye concentrations respectively (mg/L) at any time (t).  $V$  is the volume of the solution (L) and  $M$  is the mass of the used adsorbent (g).

$$\frac{C_e}{q_e} = \frac{1}{K_a Q} + \frac{1}{Q} C \quad \text{----- (6)}$$

A linear plot  $\frac{C_e}{q_e}$  against  $C_e$  will demonstrate the Langmuir adsorption isotherm's applicability. The Langmuir constants for adsorption capacity and rate of adsorption,  $K_a$  and  $Q_m$ , are determined from the slope and intercept of the plot  $\frac{C_e}{q_e}$  against  $C_e$ , respectively. The equilibrium parameter " $R_L$ ," also known as the separation factor or dimensionless constant, can be used to represent the fundamental properties of the Langmuir adsorption isotherm. It is defined by:

## 2.5 Kinetics of Biosorption

Two phases comprise biosorption kinetics: an early, extremely quick adsorption step and a subsequent, gradual adsorption stage [15]. Determining the sorbent's effectiveness requires an understanding of the biosorption kinetics. The pseudo-first order rate equation can be described as follows:

$$\frac{1}{q_t} = \frac{1}{q_1} + \frac{k_1}{q_1 t} \quad \text{----- (3)}$$

Where,

$q_1$  is the maximum biosorption capacity (mg/g); and  $q_t$  is the amount of dye biosorbed at equilibrium (mg/g);  $k_1$  is the pseudo first-order rate constant ( $\text{min}^{-1}$ ). The pseudo-second order rate equation is expressed as follows:

$$\frac{t}{q_t} = \frac{1}{k_2 q_2^2} + \frac{1}{q_2} t \quad \text{----- (4)}$$

Where,

$q_2$  is the maximum biosorption capacity (mg/g);  $q_t$  is the amount of dye biosorbed at a certain equilibrium (mg/g);  $k_2$  is the equilibrium rate constant (g/mg min).

## 2.6 Intraparticle Diffusion

The intra-particle diffusion model was further investigated as follows [16] in order to determine whether film or pore diffusion was the regulating phase in the adsorption process.

$$q_t = k_i t^{1/2} \quad \text{----- (5)}$$

Where,

$k_i$  ( $\text{mmol g}^{-1} \text{min}^{-1/2}$ ) is the intra-particle diffusion rate constant and  $q_t$  ( $\text{mmol g}^{-1}$ ) represents the amount of dye adsorbed on the adsorbents at time  $t$  (min).

## 2.7 Adsorption Isotherm

### 2.7.1 Langmuir adsorption isotherm

Langmuir adsorption isotherm was studied by surface kinetic approach [17,18]. The linearized Langmuir isotherm is

$$R_L = \frac{1}{1 + b C_i}$$

Where,

$C_i$  = dye's initial concentration and  $b$  = Langmuir constant.  $R_L$  values indicate the type of isotherm to be irreversible ( $R_L = 0$ ), favourable ( $0 < R_L < 1$ ), unfavourable ( $R_L > 1$ ) and linear ( $R_L = 1$ ).

### 2.7.2 Freundlich adsorption isotherm

The adsorption process is best described by the Freundlich isotherm model [19,20], which is the oldest known equation.

$$\log q = \log K_F + \frac{1}{n} \log C \quad \text{----- (7)}$$

The relationship between  $\log C_e$  and  $\log q_e$ , was linear, where  $n$  is the adsorption intensity and  $K_F$  is the measure of adsorption capacity (mg/g). Irreversible ( $1/n = 0$ ), advantageous ( $0 < 1/n < 1$ ) and unfavourable ( $1/n > 1$ ) isotherm types are indicated by  $1/n$  values [21]. One can compute the values of  $1/n$  and  $K_F$  based on the slope and intercept, respectively.

## 2.8 Thermodynamic Parameters

The equilibrium constant ( $K_d$ , L/g) for the adsorption of congo red on NaFRLP biosorbent was calculated at the temperatures of 298, 303, 308 and 313 K using  $K_d = \frac{q_e}{C_e}$

The following equations were used to compute the thermodynamic parameters, the enthalpy change ( $\Delta H^\circ$ ), the entropy change ( $\Delta S^\circ$ ) and Gibbs free energy change ( $\Delta G^\circ$ ).

$$\ln K_d = \frac{\Delta S^\circ}{R} - \frac{\Delta H^\circ}{RT} \quad \text{----- (8)}$$

$$\Delta G^\circ = \Delta H^\circ - T\Delta S^\circ \quad \text{----- (9)}$$

Where,

T is the absolute temperature (K) and R is the universal gas constant (8.314 J/(mol K)). The plot of  $\ln K_d$  vs  $1/T$ 's slope and intercept can be used to derive the values of  $\Delta H^\circ$  and  $\Delta S^\circ$ .

### 3. RESULTS AND DISCUSSION

#### 3.1 Characterization of NaFRLP Biosorbent

FT-IR was used to analyze the surface functional groups in the biosorbent (NaFRLP). In Fig.3, the spectrum was displayed. Peaks at 3443, 2920, 2377, 1607 and 1329  $\text{cm}^{-1}$  correspond to the vibrational frequencies of the functional groups - OH or  $-\text{NH}_2$ ,  $-\text{CH}_2$ , C=C or C=N, C=O and C-O respectively [8].

The SEM image of biosorbent in Fig.4 shows the distribution of large pores and thus endowed with greater surface area.

#### 3.2 BET Surface Area

The surface area of the biosorbent sample was determined to be  $192 \text{ m}^2\text{g}^{-1}$ , indicating a high pore volume material (Fig.5). Type IV isotherm, which is indicative of mesoporous materials and type H1 hysteresis loop are followed by adsorption by NaFRLP adsorbent. The BJH method's calculation of the pore size distribution from the desorption branch of the  $\text{N}_2$  isotherms revealed an average pore size of 18 nm, indicating the presence of mesopores in the NaFRLP adsorbent.

#### 3.3 Effect of Operational Parameters

##### 3.3.1 Effect of variation of Initial dye concentration

By altering the dye beginning concentration while holding all other variables constant, the impact of the starting concentration was investigated. "The maximum percentage removal was found at an ideal initial dye concentration of 100 mg/L on NaFRLP. According to the experimental measurements of the extent of dye removal, the rate of dye removal lowers as the initial dye concentration rises and vice versa. This is because the creation of a monolayer at the lower initial concentration of dye on the adsorbent

surface greatly inhibits the formation of subsequent layers of dye species. The variation can be shown as seen in Fig.6. This suggests that the adsorption of dye may either induce particles to agglomerate and reduce the number of active sites required for adsorption or it may limit dyes access to the original pores" [22].

##### 3.3.2 Effect of Agitation speed

When the agitation speed was increased up to 200 rpm, an improvement in the adsorption capacity and % removal of dye using NaFRLP as shown in Fig.7. Beyond that, the adsorption capability and % removal of dye diminish. The film boundary layer encircling the particles and consequently, their adsorption capability are decreased when the degree of agitation speed increases. As the speed of the agitation increases, some of the dye that has adsorbed on the leaf powder surface desorbe because of centrifugal force, which causes the bound dye to desorbe [23]. At an agitator speed of 200 rpm, the maximum adsorption capacity is reached and the greatest percentage of dye removed under these conditions is 95.58%.

##### 3.3.3 Effect of adsorbent dosage

With a constant initial congo red concentration of 100 mg/L and an agitation period of 90 min at 298 K, the NaFRLP dosage was varied from 0.1 to 2 g/L. The impact of adsorbent dosage on the percentage of dye removed under equilibrium conditions is depicted in Fig. 8. It was found that changing the dosage of the adsorbent affected the amount of dye adsorbed. The adsorption of congo red increased quickly upon increasing the adsorbent dosage from 0.1 to 1 g/L. However, an additional increase in the dosage of NaFRLP was insufficient to sufficiently boost its adsorption capability. The adsorption sites in NaFRLP are connected to the rise in the % dye adsorption. The dye molecules compete with one another for adsorption at limited adsorption sites at lower adsorbent dosages. But as NaFRLP concentration increases, more adsorption sites become available, which encourages adsorption and raises the percentage of dye removal [24].

##### 3.3.4 Effect of Contact time

The duration of the contact has a significant impact on the adsorption efficiency. The term "contact time" refers to the amount of time required for the adsorption process to reach equilibrium, or the point at which no further

variations in the adsorptive concentration are seen. The variations in the adsorbent distinctive qualities determine this contact time. When removing congo red from aqueous solutions at a concentration of 100 mg/L, an adsorbent dosage of 1 g/L and a temperature of 313 K, contact

times were adjusted between 10 and 90 minutes to maximize the uptake of congo red (Fig. 9). The findings obtained from the adsorption capacity of congo red on to NaFRLP demonstrated that the biosorption increases with increase in contact time until it reached equilibrium [25].

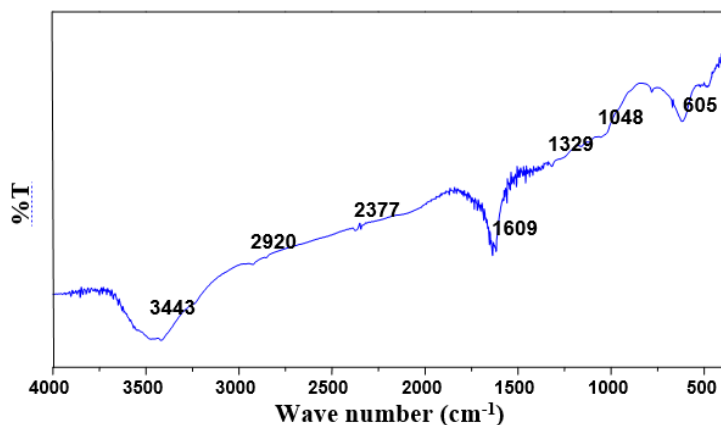


Fig. 3. FT-IR spectrum of NaFRLP biosorbent

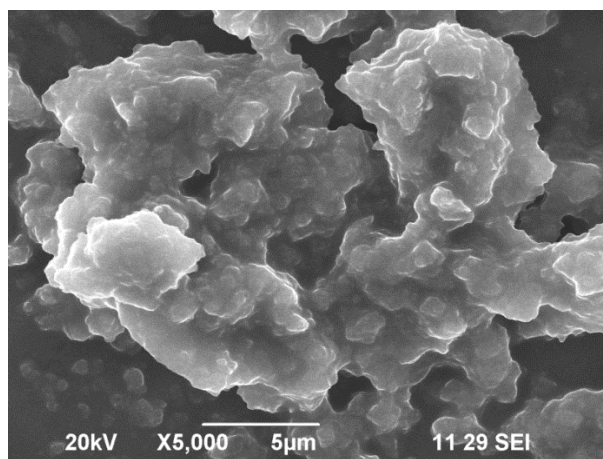


Fig. 4. SEM image of NaOH treated *Ficus Racemosa* Leaf Powder (NaFRLP)

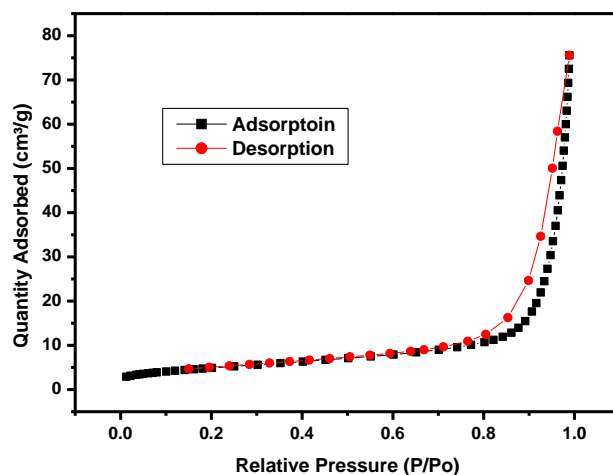
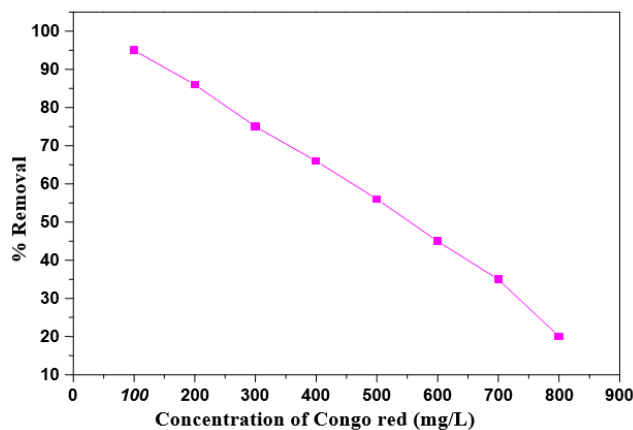
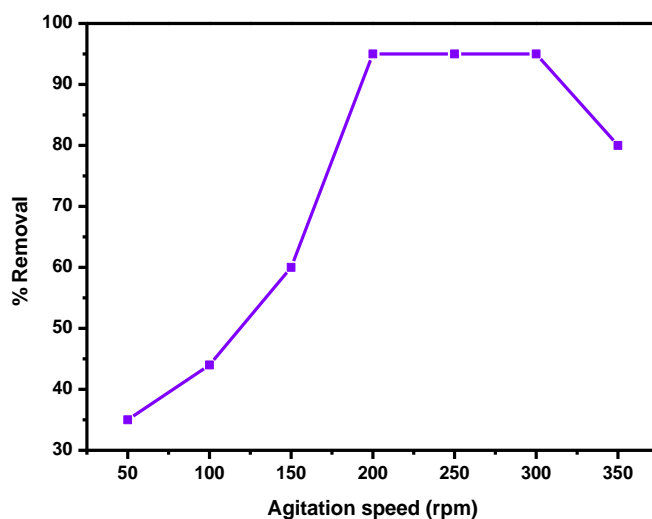


Fig. 5. BET surface area



**Fig. 6. Effect of Initial dye concentration on percentage removal of Congo red**  
[Adsorbent dose ( $w$ ) = 1 g/L, Agitation time  $t$  = 90 min, Agitation speed = 200 rpm, Temperature = 313 K]



**Fig. 7. Effect of Agitation speed**  
[Initial dye concentration = 100 mg/L, Agitation time  $t$  = 90 min, Temperature = 313 K]

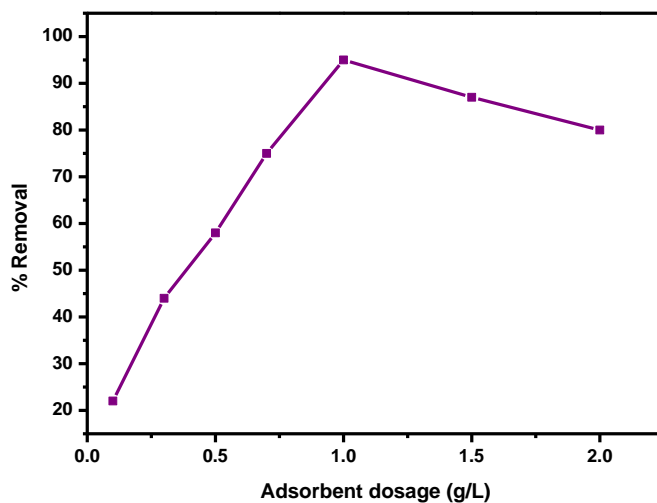


**Fig. 8. Effect of Adsorbent dosage on % removal of Congo red**  
[Initial dye concentration = 100 mg/L, Agitation time  $t$  = 90 min, Agitation speed = 200 rpm, Temperature = 313 K]

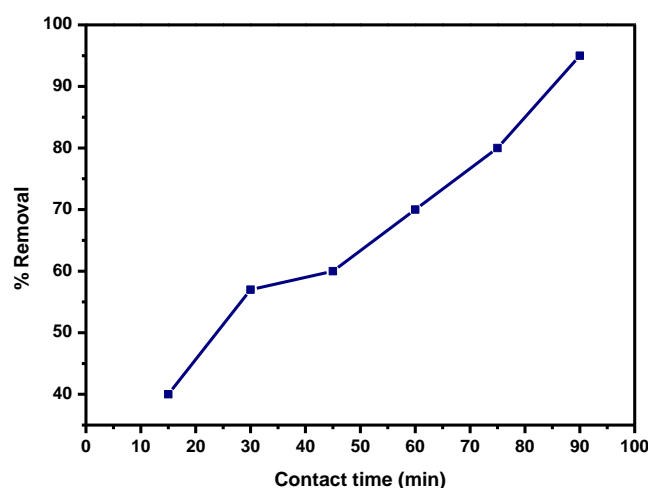


**Fig. 9. Effect of Contact time on % removal of Congo red**

[Initial dye concentration = 100 mg/L, Adsorbent dosage = 1 g/L, Agitation speed = 200 rpm, Temperature = 313 K]

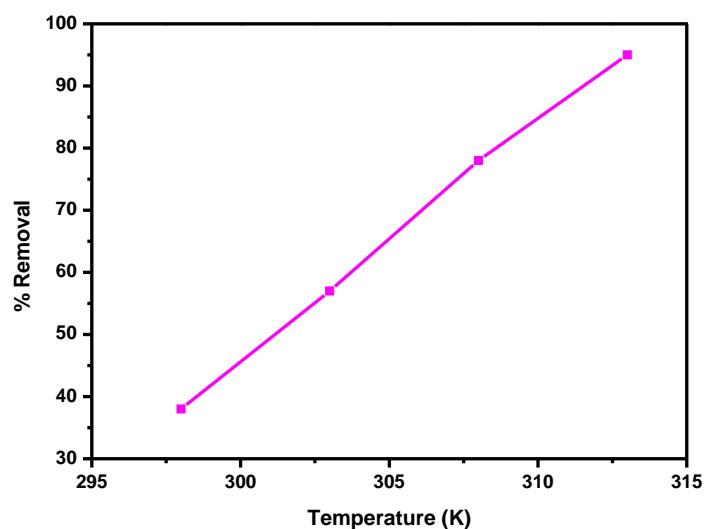


**Fig. 10. Effect of Temperature on % removal of Congo red**

[Initial dye concentration = 100 mg/L, Adsorbent dosage = 1 g/L, Agitation speed = 200 rpm, Contact time = 90 min]

### 3.3.5 Effect of Temperature

Using a constant dye concentration of 100 mg/L and a 90-minute contact time, the effect of temperature on the adsorption of congo red by NaFRLP was investigated at 298, 303, 308 and 313 K (Fig.10). "The adsorption process is endothermic, as evidenced by the observation that the adsorption capabilities of congo red increased as the solution temperature increased from 298 to 313 K. The enhanced rate at which dye molecules diffuse through the external boundary layer and into the adsorbent's internal pores may be the cause of the temperature-dependent increase in adsorption capacity" [26].

### 3.4 Adsorption Isotherm

The adsorption of an adsorbate on a uniform, flat surface of an adsorbent and monolayer adsorption on a surface with a finite number of identical sites are both described by the Langmuir isotherm. In contrast to the Langmuir model, the adsorption of an adsorbate onto the heterogeneous surface of an adsorbent was described by the Freundlich model. Table 1 provides a summary of the isotherm parameters for the adsorption of congo red. Findings suggested that the higher correlation coefficient ( $R^2$ ) values (Figs.11 and 12) demonstrated a good agreement between the Langmuir model

and the adsorption of Congo red on NaFRLP. These results show that the adsorption process is uniform. A favorable adsorption process was indicated by the values of  $R_L$ , which ranged from 0 to 1 [27].

### 3.5 Adsorption Kinetics

Adsorption kinetics is crucial for understanding the underlying principles and assessing how well

a particular adsorbent performs [28]. According to Hameed [29], kinetic modeling is typically employed to look at the mechanism of adsorption as well as possible rate-controlling mechanisms including chemical reactions and mass transfer. Two popular models: pseudo-first order and pseudo-second order models were used in the present work to simulate the kinetics of Congo red adsorption on NaFRLP.

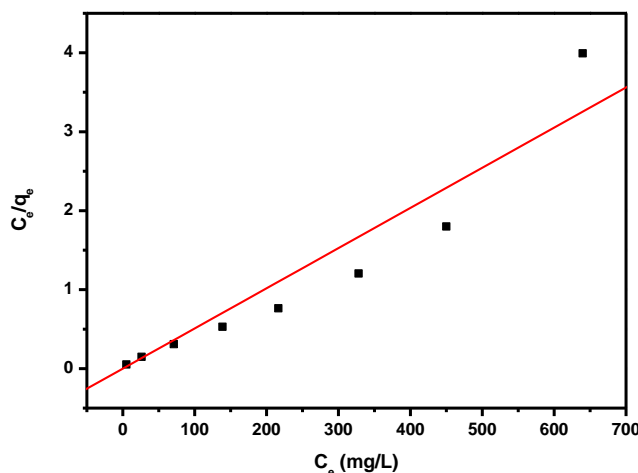


Fig. 11. Linear plot of Langmuir isotherm for adsorption of Congo red on NaFRLP

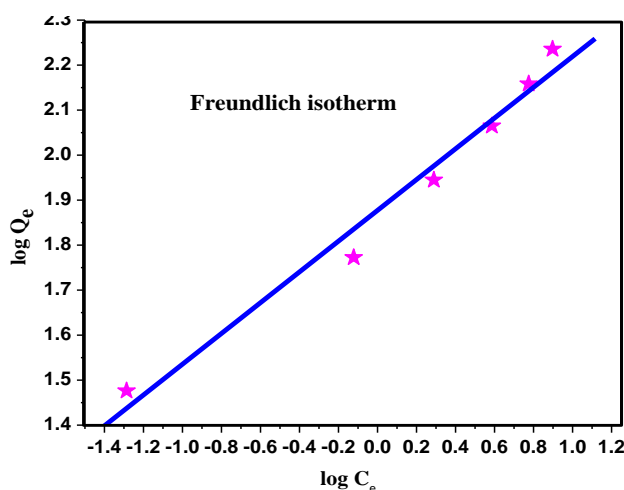


Fig. 12. Linear plot of Freundlich isotherm for adsorption of Congo red on NaFRLP

Table 1. Parameters of various isotherms for Congo red adsorption by NaFRLP

Isotherm	Parameters	Congo red
Langmuir	$R^2$	0.962
	$Q_m$	9.612
	$R_L$	0.0276
	$K_a$	3.512
Freundlich	$R^2$	0.906
	$n$	4.2016
	$K_f$	1.5204

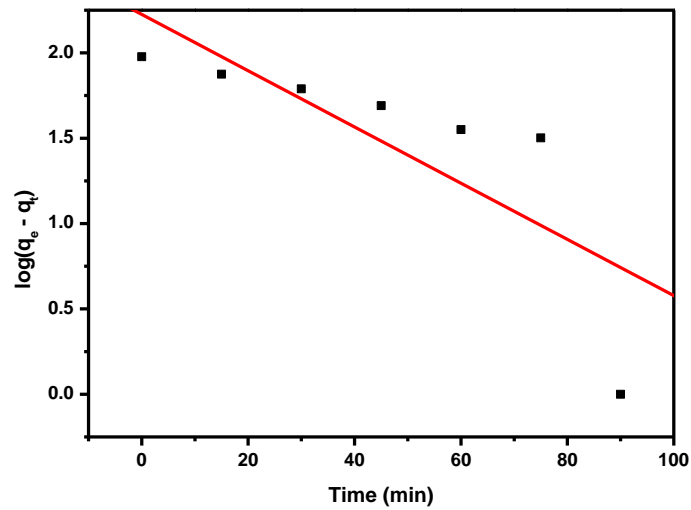


Fig. 13. Pseudo first order kinetics for adsorption of Congo red on NaFRLP

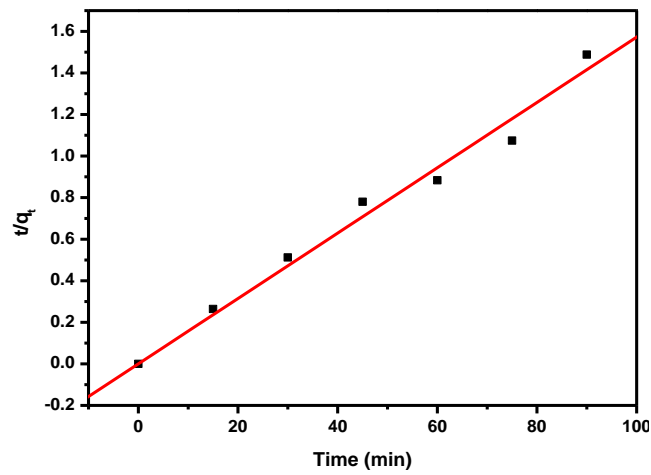


Fig. 14. Pseudo second order kinetics for adsorption of Congo red on NaFRLP

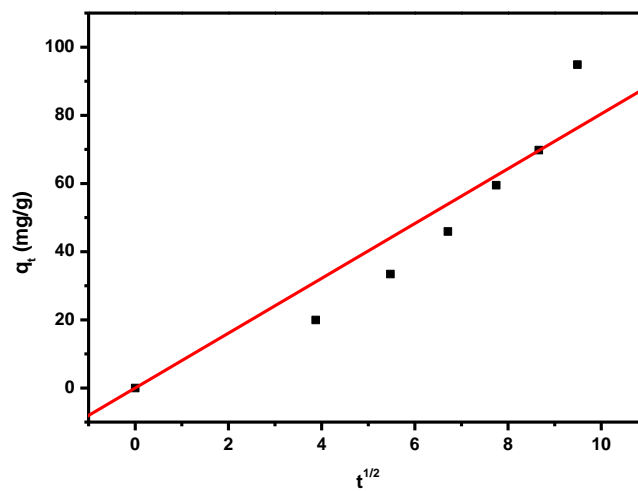


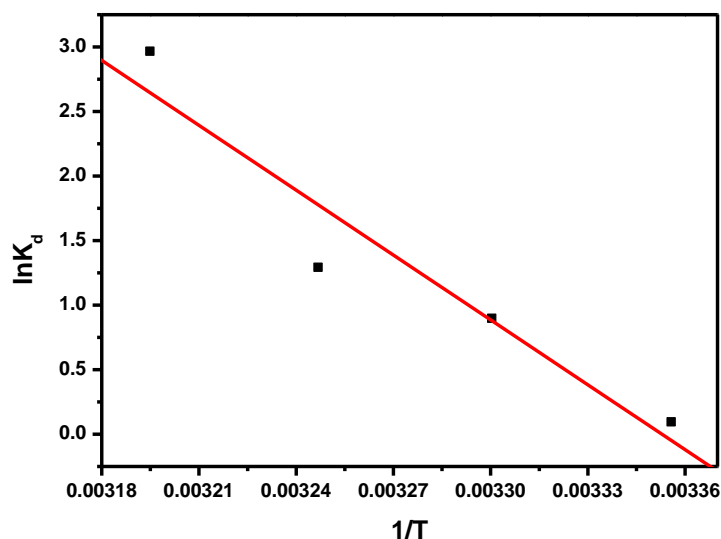
Fig. 15. Linear plot of Intra particle diffusion

**Table 2. Parameters of adsorption kinetic models of Congo red on NaFRLP**

Adsorption kinetic model	Parameter	Congo red
Pseudo-First order	R <sup>2</sup>	0.334
	k <sub>1</sub> (min <sup>-1</sup> )	0.0184
	q <sub>e</sub> (mg/g)	1.0876
Pseudo-Second order	R <sup>2</sup>	0.960
	k <sub>2</sub> (min <sup>-1</sup> )	0.0408
	q <sub>e</sub> (mg/g)	95.5367
Intra particle diffusion model	h	0.1863
	R <sup>2</sup>	0.983
	K <sub>diff</sub>	0.210
	C	0.099

**Table 3. Thermodynamic parameters for adsorption of Congo red on NaFRLP**

Temperature (°C)	ΔG° (kJ/mol <sup>-1</sup> )	ΔH° (kJ mol <sup>-1</sup> )	ΔS° (JK <sup>-1</sup> mol <sup>-1</sup> )	K <sub>d</sub>	
Congo red	298	-1.218	241.42	79.86	0.4083
	303	-2.66			0.9140
	308	-3.312			3.6451
	313	-7.712			19.439

**Fig. 16. Van't Hoff plot for the adsorption of Congo red on NaFRLP**

The Congo red kinetic plots on NaFRLP for the pseudo-first order model and pseudo-second order model are shown in Figs.13 and 14 respectively. Table 2 displays the kinetic parameters that were determined. "Since the simulated curves fit the experimental data better, the calculated  $q_{e,calc}$  values were closer to the experimental ones ( $q_{e,expt}$ ) and the pseudo-second order model had higher correlation coefficients than the pseudo-first order model. All of these findings suggest that the rate-limiting step for NaFRLP was chemical adsorption" [30]. The intra-particle diffusion curve for Congo red adsorption on NaFRLP is displayed in Fig.15.

Multiple linear portions are seen across the plot, indicating that two or more stages are affecting the adsorption [31]. This can be illustrated as follows: The first, steeply sloping section depicts the immediate diffusion stage, during which a significant number of dye molecules from the bulk phase were quickly adsorbed by NaFRLP surface functional groups. The dye molecules prepared to enter the adsorbent pores after nearly all of the external active sites were occupied. The interior surface of the pores then arose in the second stage and adsorbed the dye molecules. The third section showed that the equilibrium state had finally been reached

because the intra-particle diffusion rate constants were almost zero. According to kinetic investigations, the adsorption processes were impacted by intra-particle diffusion as well as the chemical chelating reaction between dye molecules and the adsorbent active sites [30].

### 3.6 Thermodynamic Parameters

At 298, 303, 308 and 313 K, the Gibbs free energy change ( $\Delta G^\circ$ ) for congo red adsorption was determined to be -1.218, -2.66, -3.312 and -7.712 kJ/mol respectively (Table 3). For congo red, negative  $\Delta G^\circ$  values were recorded at all examined temperatures, indicating the process viability and spontaneous nature of adsorption. Additionally, when temperature increased, the  $\Delta G^\circ$  values reduced, suggesting that the degree of spontaneity and feasibility of congo red adsorption was increased. For the adsorption of congo red, the  $\Delta H^\circ$  parameter was found to be 79 kJ/mol. The endothermic nature of the adsorption process was further supported by the positive values of  $\Delta H^\circ$ . The chemisorption process is indicated by a heat of adsorption value between 40 and 400 kJ/mol [32]. Therefore, congo red adsorption on NaFRLP is chemical in nature. For congo red adsorption, the  $\Delta S^\circ$  parameter was determined to be 79.86 (J/(mol K)). The solid-liquid interface degrees of freedom appeared to grow during the adsorption process, based on the positive values of  $\Delta S^\circ$ . The coordinated water molecules were replaced by dyes during the adsorption process, which made the adsorbent-adsorbate system more random [33]. Fig.16 shows the Van't Hoff plot for the congo red adsorption on NaFRLP.

### 4. CONCLUSION

The use of *Ficus racemosa* fallen leaf powder treated with NaOH (NaFRLP) as a biosorbent to remove congo red dye from industrial waste water has been investigated. The biosorbent was characterized by FT-IR and SEM analysis. The biosorbent was found to include mesoporous particles based on surface area analysis (BET). According to batch adsorption experiments, the percentage of congo red removed increases with an increase in adsorption time and decreases with an increase in dye concentration. For the elimination of congo red, NaFRLP was found to be an effective adsorbent up to a concentration range of 100 mg/L. The Langmuir isotherm best fits the adsorption data. Thermodynamic analysis of the batch adsorption investigations revealed that the congo red adsorption on NaFRLP was

endothermic and that all the other processes were spontaneous. Therefore, the most suitable biosorbent for the effective removal of congo red is NaFRLP.

### COMPETING INTERESTS

Author has declared that no competing interests exist.

### REFERENCES

1. Robson C. Oliveira, Mauricio C. Palmieri and Oswaldo Garcia Jr. Progress in biomass and bio energy Production, In Tech. 2011;151-176.
2. Ozdemir S, Kilinc E, Poli A, Nicolaus B, & Guven K, Biosorption of Cd, Cu, Ni, Mn and Zn from aqueous solutions by thermophilic bacteria, *Geobacillus toebii* sub.sp. decanicus and *Geobacillus thermoleovorans* sub.sp. stromboliensis: Equilibrium, kinetic and thermodynamic studies, Chemical Engineering Journal. 2009;152(1):195-206.
3. Al Prol AE, El-Azzem MA, Amer A, El-Metwally ME, El-Hamid HTA, El-Moselhy KM, Adsorption of Cadmium (II) ions from aqueous solution on to mango leaves, Asian Journal of Physical and Chemical Sciences. 2017; 2:1–11.
4. Tran HN, You SJ, Hosseini-Bandegharaei A, Chao HP, Mistakes and inconsistencies regarding adsorption of contaminants from aqueous solutions: a critical review, Water Res. 2017; 120:88–116.
5. Guerrero-Coronilla I, Morales-Barrera L, Villegas-Garrido TL, Cristiani-Urbina E, Biosorption of amaranth dye from aqueous solution by roots, leaves, stems and the whole plant of *E. crassipes*, Environ. Eng. Manag. J. 2014; 14:1917–1926.
6. Gupta N, Kushwaha AK, Chattopadhyaya MC, Adsorption studies of Cationic dyes on to Ashoka (*Saracaasoca*) leaf powder, J. Taiwan Inst. Chem. Eng. 2012;43:604–613.
7. Jain SN, Gogate PR, Adsorptive removal of acid violet 17 dye from wastewater using biosorbent obtained from NaOH and H<sub>2</sub>SO<sub>4</sub> activation of fallen leaves of *Ficus racemosa*, J. Mol. Liq. 2017;243:132–143.
8. Sujitha Ravulapalli, Ravindhranath Kunta, Defluoridation studies using active carbon derived from the barks of *Ficus racemosa* plant, Journal of Fluorine Chemistry. 2017;193:58–66.

9. Jain SN, Gogate PR, NaOH treated dead leaves of *Ficus racemosa* as an efficient biosorbent for Acid Blue 25 removal, International Journal of Environmental Science and Technology. 2017; 14:531-542.
10. Youssef Aoulad El Hadj Ali, Abdoulaye Demba N'diaye, Driss Fahmi Mohamed Sid'Ahmed Kankou, Mostafa Stitou, Adsorption of congo red from aqueous solution using typha australis leaves as a low cost adsorbent, Journal of Environmental Treatment Techniques. 2021; 9(2):534-539.
11. Aisha Kitemangu, Maheswara Rao Vegi and Nyemaga Masanje Malim, Biosorption of congo red dye from aqueous solution using adsorbent prepared from vanguardia infausta fruit pericarp, Hindawi Adsorption Science & Technology Volume.2023;17.Article ID 4319053.
12. Maria Harja, Gabriela Buema, Daniel Bucur, Recent advances in removal of Congo Red dye by adsorption using an industrial waste, Scientific reports. 2022; 12:6087.
13. Mohammad Foroughi-dahr, Hossein Abolghasemi, Mohamad Esmaili, Alireza Shojamoradi and Hooman Fatoorehchi, Fixed-bed adsorption of Congo red on tea waste in the presence of Fe<sub>2</sub>O<sub>3</sub> nanoparticles: An experimental and modeling study, Journal of Petroleum Science and Technology.2013;3(2):35-44.
14. Material Safety Data Sheet Congo red MSDS.Available:[http://www.sciencelab.com/xMSDS-Congo\\_red-9927502](http://www.sciencelab.com/xMSDS-Congo_red-9927502).
15. Tunali S, Cabuk A, Akar T. Removal of Lead and Copper Ions from Aqueous Solutions by Bacterial Strain Isolated from Soil, Chemical Engineering Journal. 2006; 115(3):203-211.
16. Langmuir I, The Constitution and Fundamental Properties of Solids and Liquids. Part I. Solids. Journal of the American Chemical Society.1916; 38:2221-2295.
17. Aksu Z, Donmez D, A comparative study on the biosorption characteristics of some yeasts for Remazol Blue reactive dye, Chemosphere.2003;50:1075-1083.
18. Elisane Longhinotti, Fabíola Pozza, Lígia Furlan, Maria de Nazaré de M. Sanchez, Marilene Klug, Mauro CM. Laranjeira and Valfredo T. Fávere, J. Braz. Chem. 1998;9(5).
19. Freundlich HM. Über die adsorption in losungen, Zeitschrift für Physikalische Chemie. 1906; 57A:385–470.
20. Hall KR, Eagleton LC, Acrivos A, Vermevlem T, Pore and Solid-Diffusion Kinetics in Fixed-Bed Adsorption under Constant-Pattern Conditions. Industrial Engineering Chemistry Fundamentals. 1966;5: 212-223.
21. Ho YS, Citation review of Lagergren kinetic rate equation on adsorption reactions, Scientometrics.2004;59:171-177.
22. Montanher SF, Oliveira EA, Rollemberg MC, Hazard J. Mater. 2005;B117:207-211.
23. Crini G, Peindy HN, Gimbert F, Robert C, Removal of C. I. Basic Green 4 (Malachite Green) from Aqueous Solutions by Adsorption Using Cyclodextrin-based Adsorbent: Kinetic and Equilibrium Studies, Separation and Purification Technology.2007;53:97–110.
24. Xu X, Li Q, Cui H, Pang J, Sun L, An H, Zhai J, Adsorption of fluoride from aqueous solution on magnesia-loaded fly ash cenospheres desalination.2011;272:233–239.
25. Ramanaiah SV, Mohan SV, Rajkumar B, Sarma PN, Monitoring of Fluoride Concentration in Groundwater of Prakasham District in India: Correlation with Physico-Chemical Parameters, Journal of Environmental Science & Engineering. 2006;48:129–134.
26. Ismat H. Ali and Alrafai HA, Kinetic, isotherm and thermodynamic studies on biosorption of chromium(VI) by using activated carbon from leaves of *Ficus nitida*, Chemistry Central Journal. 2016;10:36.
27. Chen N, Zhang Z, Feng C, Li M, Zhu D, Chen R, Sugiura N, An excellent fluoride sorption behavior of ceramic adsorbent, J. Hazard. Mater. 2010;183:460–465.
28. Qiu H, Lv L, Pan B, Zhang Q, Zhang W, Zhang, Q, Critical review in adsorption kinetic models, Journal of Zhejiang Univ.Sci. A.2009;10:716–724.
29. Hameed BH. Spent tea leaves: A new non conventional and low cost adsorbent for removal of basic dye from aqueous solutions. *J Hazard Mater* 2009; 161:753-759.
30. Repo E, Warchol JK, Kurniawan TA, Sillanpää M, Adsorption of Co(II) and Ni(II) by EDTA- and/or DTPA-modified chitosan: kinetic and equilibrium modeling. Chem. Eng. J. 2010;161:73–82.

31. Chen Y, Hu J, Wang J, Kinetics and thermodynamics of Cu(II) biosorption on to a novel magnetic chitosan composite bead Environ. Technol. 2012;33:2345–2351.
32. Unlu N, Ersoz M, Removal of heavy metal ions by using dithiocarbamated-sporopollenin, Sep. Purif. Technol. 2007;52:461–469.
33. Baraka A, Hall PJ, Heslop MJ, Preparation and characterization of melamine–formaldehyde–DTPA chelating resin and its use as an adsorbent for heavy metals removal from wastewater, React. Funct. Polym. 2007;67:585–600.

© Copyright (2024): Author(s). The licensee is the journal publisher. This is an Open Access article distributed under the terms of the Creative Commons Attribution License (<http://creativecommons.org/licenses/by/4.0>), which permits unrestricted use, distribution, and reproduction in any medium, provided the original work is properly cited.

*Peer-review history:*

*The peer review history for this paper can be accessed here:*  
<https://www.sdiarticle5.com/review-history/113844>